



Comparative study of variations in mechanical stress and strain of human blood vessels: mechanical reference for vascular cell mechano-biology

Shaoxiong Yang¹ · Xiaobo Gong¹ · Yingxin Qi² · Zonglai Jiang²

Received: 16 October 2018 / Accepted: 31 August 2019 / Published online: 7 September 2019
© Springer-Verlag GmbH Germany, part of Springer Nature 2019

Abstract

The diseases of human blood vessels are closely associated with local mechanical variations. A better understanding of the quantitative correlation in mechanical environment between the current mechano-biological studies and vascular physiological or pathological conditions *in vivo* is crucial for evaluating numerous existing results and exploring new factors for disease discovery. In this study, six representative human blood vessels with known experimental measurements were selected, and their stress and strain variations in vessel walls under different blood pressures were analyzed based on nonlinear elastic theory. The results suggest that conventional mechano-biological experiments seeking the different biological expressions of cells at high/low mechanical loadings are ambiguous as references for studying vascular diseases, because distinct “site-specific” characteristics appear in different vessels. The present results demonstrate that the inner surface of the vessel wall does not always suffer the most severe stretch under high blood pressures comparing to the outer surface. Higher tension on the outer surface of aortas supports the hypothesis of the outside-in inflammation dominated by aortic adventitial fibroblasts. These results indicate that cellular studies at different mechanical niches should be “disease-specific” as well. The present results demonstrate considerable stress gradients across the wall thickness, which indicate micro-scale mechanical variations existing around the vascular cells, and imply that the physiological or pathological changes are not static processes confined within isolated regions, but are coupled with dynamic cell behaviors such as migration. The results suggest that the stress gradients, as well as the mechanical stresses and strains, are key factors constituting the mechanical niches, which may shed new light on “factor-specific” experiments of vascular cell mechano-biology.

Keywords Mechanical stress and strain · Stress gradient · Mechanical niche · Vascular cell mechano-biology

1 Introduction

It is getting to know that mechanical environments such as stresses and strains play crucial roles in the comprehensive remodeling behaviors of human blood vessels, which are important in both regular physiological functions and pathological dysfunctions. For a better understanding of the

mechanism that couples biological and mechanical physics from cellular to tissue scales, numerous *in vitro* mechano-biological experiments for vascular cells have been reported (Wells 2008; Humphrey et al. 2014; Sears and Kaunas 2016). However, from the viewpoint of the mechanical niches of resident cells (Ingber 2003; Chen 2008), to what extent current studies *in vitro* on cellular mechano-transduction can correlate quantitatively to vascular physiological or pathological conditions *in vivo* is a critical question to ask for evaluating existing results and exploring new factors for disease discovery.

Cells as machines respond to their mechanical stimuli appropriately (Sheetz and Yu 2018). According to the classical stress-growth theory (Fung 1991), none of the mechano-biological responses of cells is proportional to even a single mechanical stimulus. Blood vessels exhibit different geometries, material properties, loadings, and residual stresses

✉ Xiaobo Gong
x.gong@sjtu.edu.cn

¹ Key Laboratory of Hydrodynamics (Ministry of Education), Department of Engineering Mechanics, School of Naval Architecture, Ocean and Civil Engineering, Shanghai Jiao Tong University, Shanghai, China

² Institute of Mechanobiology and Biomedical Engineering, School of Life Sciences and Biotechnology, Shanghai Jiao Tong University, Shanghai, China

in vivo at different arterial locations (Saini et al. 1995; Holzapfel et al. 2000; Kamenskiy et al. 2014), which makes the mechanical environments of vascular cells complicated (Azar et al. 2018). Although several mechanical factors, such as the stress, strain, and stiffness of substrates, have been extensively reported as crucial parameters in mechano-biological studies, a fundamental standard for the guidance of mechanical stimuli is still lacking (Kumar et al. 2017). The variations of the mechanical stress and strain have not been systematically evaluated and discussed for the arterial system under healthy and high blood pressure conditions either.

Clinical investigations measured the in vivo pulsatile expansion of the arterial wall and relative circumferential strain (Isnard et al. 1989; Boutouyrie et al. 1992), the results of which were used to guide in vitro cell stretching (Anwar et al. 2012). However, the residual stresses in vascular tissues compromise the strain measurement accuracy, so that the observed relative strain deviates substantially from the real strain with respect to the stress-free configuration (Chuong and Fung 1986). Nonlinear solid mechanics provides a theoretical way for quantifying these important mechanical factors onsite at the vascular wall (Holzapfel 2000; Humphrey 2002). By means of biaxial extension testing and histological evaluation, Kamenskiy et al. (2014) verified the hypothesis that the mechanical properties and microstructures of human arteries are dependent on specific locations and physiological functions. They estimated the material parameters and geometries of six major arteries, so that the in vivo stress/strain distributions are ready for detailed analysis. It has been reported that stress gradients within vascular tissues play important roles in cell movement (Lo et al. 2000), but their variations within three-dimensional vessel walls remain to be studied.

With the development of numerical methods for vascular mechanics, it is possible to predict the stress state in blood vessels more reliably with experimentally measured material parameters. But, over the past decades, main applications of these simulations are to develop artery-specific surgical therapies or medical devices for cardiovascular diseases (Gasser et al. 2002, 2010; Lally et al. 2005; Humphrey and Holzapfel 2012; Pierce et al. 2015), and the mechanical niches of vascular cells require more discussions. As an example, Sommer et al. (2018) recently investigated the biomechanical differences between subclavian and common iliac arteries under extension, inflation and torsion, which suggested that the high stiffness of the subclavian arteries explains the wall vulnerability during vascular operations. Their study focused on improving surgical interventions, rather than exploring the micromechanical environments for cells.

In this study, we tried to specify mechanical references of representative human vessels for the study of vascular cell mechano-biology. The contents are presented as follows. In Sect. 2, six human blood vessels including segments of

the aortas and major branches are selected for stress analysis, before which the analytical methods are illustrated. In Sect. 3, the variations of the mechanical stress/strain distributions and stress gradients in the vessel walls under different blood pressures are illustrated. In Sect. 4, the biomechanical characteristics of blood vessels on cellular mechano-transduction are discussed, and a novel factor is proposed. Finally, conclusions are presented in Sect. 5.

2 Materials and methods

2.1 Blood vessel geometries and constitutive relations

Benefiting from the available mechanical experiments (Kamenskiy et al. 2014), six human blood vessels without severe diseases were selected, as illustrated in Fig. 1. They are thoracic (TA) and abdominal (AA) aortas, and common iliac (CIA), subclavian (SA), renal (RA), and common carotid (CCA) arteries. These blood vessels are representatives for the investigation of the mechanical environments in the vessel walls and for studying and comparing the characteristics of human blood vessels at different locations.

In this study, blood vessels were modeled as thick-wall straight tubes with residual stresses. An anisotropic constitutive formulation consisting of four exponential functions

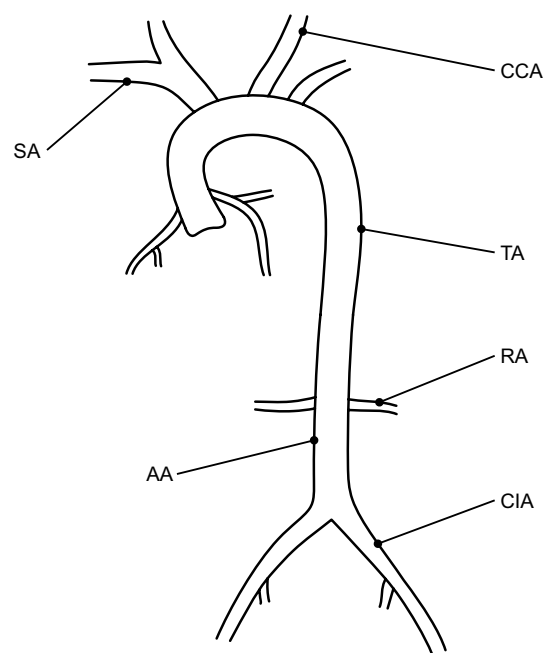


Fig. 1 Human aortas and major branches selected for stress analysis in this study. TA thoracic aorta, AA abdominal aorta, CIA common iliac artery, SA subclavian artery, RA renal artery, CCA common carotid artery

was used to describe the nonlinear mechanical behaviors of vessel walls (Kamenskiy et al. 2014):

$$W(\mathbf{C}, \mathbf{M}_i) = \frac{c_0}{2} (I_1 - 3) + \sum_{i=1}^4 \frac{m_i c_{i1}}{4c_{i2}} \left\{ \exp \left[c_{i2} (I_{i4} - 1)^2 \right] - 1 \right\}. \tag{1}$$

Here, I_1 is the first invariant of the right Cauchy–Green tensor \mathbf{C} ; $\mathbf{M}_i = \mathbf{a}_i \otimes \mathbf{a}_i$ is the tensor product of unit vector $\mathbf{a}_i = [0 \sin \gamma_i \cos \gamma_i]^T$, $i = 1, 2, 3, 4$; $I_{i4}(\mathbf{C}, \mathbf{a}_i) = \mathbf{a}_i \cdot \mathbf{C} \mathbf{a}_i$ is the pseudo-invariant of \mathbf{C} and \mathbf{M}_i ; c_0 , c_{i1} , and c_{i2} are material parameters with $c_{31} = c_{41}$ and $c_{32} = c_{42}$. In addition, the exponential terms in Eq. (1) only contribute when $I_{i4} > 1$ (Holzapfel et al. 2000), therefore:

$$m_i = \begin{cases} 1 & \text{when } I_{i4} > 1 \\ 0 & \text{when } I_{i4} \leq 1 \end{cases}. \tag{2}$$

Referring to the work of Kamenskiy et al. (2014), the inner and outer radii in stress-free configuration, opening angle, and constitutive parameters for the six blood vessels are summarized in Table 1.

The opening angle α in Table 1 is used to quantify the residual stress in blood vessels, which is defined by two radii drawn from the midpoint of the inner wall to the tips of the inner wall (Fung 1993). It should be noted that the opening angle data are normally not available especially when the complicated three-dimensional geometries or multi-layer structures of blood vessels are considered. Some studies in the literature have reported to estimate the geometries and material parameters of vessel walls with non-invasively measured pressures and medical images (Masson et al. 2011; Wang et al. 2017). However, problems of non-uniqueness might arise when too many unknown parameters need to be fitted or the unknown parameters are sensitive to small changes of the in vivo measured data (Masson et al. 2011).

The axial in situ stretch λ_z is used to quantify the magnitude of the axial loading, which is defined as the ratio of axial length of a vessel segment in situ to its ex situ axial length. As shown in Table 2, the λ_z of AA, CIA,

and CCA is collected from experimental measurements (Delfino et al. 1997; Schulze-Bauer et al. 2003; Holzapfel et al. 2007), and the λ_z of TA is assumed to be the same as that of AA, and the λ_z of SA and RA is not available in the experimental research and is assumed to be 1.1.

Hemodynamic studies demonstrate that the variation range of pulse blood pressure exhibits no obvious change along the human aorta (Boileau et al. 2015). Therefore, the six blood vessels in this study are assumed to experience the same systolic and diastolic pressures. According to Chobanian et al. (2003), the blood pressures adopted in the stress analysis are divided into five stages: normal blood pressure ($P = 10.8$ kPa), prehypertension ($P = 13.2$ kPa), stage 1 hypertension ($P = 15.0$ kPa), stage 2 hypertension ($P = 16.7$ kPa), and stage 3 hypertension ($P = 17.7$ kPa).

2.2 Analytical method

Based on nonlinear solid mechanics, the stress responses of the blood vessels are described, and the semi-analytical method of solving the equilibrium equations with proper boundary conditions is provided. More details are illustrated in Appendices 1 and 2.

Table 2 The axial in situ stretch (λ_z) for the selected blood vessels

	N	λ_z	References
TA	–	1.196	–
AA	7	1.196	Holzapfel et al. (2007)
CIA	9	1.071	Schulze-Bauer et al. (2003)
SA	–	1.1	–
RA	–	1.1	–
CCA	–	1.1	Delfino et al. (1997)

Number of donors for each blood vessel is signified by n . Symbol “–” denotes that the data are not available

Table 1 The inner (R_i) and outer (R_o) radii in stress-free configuration, opening angle (α), and constitutive parameters for the selected blood vessels (Kamenskiy et al. 2014)

	Age	R_i (mm)	R_o (mm)	α (°)	C_0 (kPa)	C_{11} (kPa)	C_{12}	C_{21} (kPa)	C_{22}	C_{31} (kPa)	C_{32}	γ (°)
TA	57	30.59	33.55	117.0	30.20	8.09	11.11	16.76	0.40	0.20	15.40	48.53
AA	43	22.61	24.55	132.0	21.75	1.46	13.29	4.13	5.09	2.35	15.25	27.49
CIA	43	11.58	12.90	114.0	12.56	6.02	13.85	8.75	1.38	2.57	11.93	32.97
SA	43	7.99	8.90	88.4	23.91	3.83	2.54	16.58	2.75	3.42	6.39	46.39
RA	82	4.39	5.25	68.2	4.98	54.22	9.83	7.62	9.24	13.91	18.64	46.54
CCA	60	5.38	6.67	77.0	15.82	2.19	5.24	6.04	2.56	2.20	7.41	40.67

All the donors are male, and each blood vessel selected here was from a single donor

3 Results

3.1 Effects of residual stress on stress distributions

Figure 2 illustrates the distributions of circumferential stresses $\sigma_{\theta\theta}$ across the vessel walls under normal blood pressure. In order to investigate the effects of residual stress on the stress distributions, the results with residual stress (w/RS) and those without residual stress (w/o RS) were compared. As shown in the figure, higher stress concentration is observed at the inner wall when the residual stress is not taken into account. The existence of the residual stress substantially alters the stress distributions in the vessel walls, resulting in a decrease in the $\sigma_{\theta\theta}$ at the inner wall and an increase in the $\sigma_{\theta\theta}$ at the outer wall.

When the residual stress is taken into account, the stress concentrations at the inner walls of TA and AA are alleviated, however, the $\sigma_{\theta\theta}$ at the outer walls exhibits a significant increase by more than 170.0% (up to 100.0 kPa). For CIA, SA, and RA, the results of the $\sigma_{\theta\theta}$ along the radial direction with residual stress increase linearly. For CCA, the residual stress helps to form a uniform stress

distribution across the vessel wall, and the magnitude of the $\sigma_{\theta\theta}$ is around 50.0 kPa.

3.2 Stress distributions

Figure 3 illustrates the distributions of circumferential stresses $\sigma_{\theta\theta}$ across the vessel walls at different hypertension stages. The stresses in TA, AA, and CIA exhibit an increase in the radial direction. The maximum stress occurring at the outer wall of AA exceeds 223.0 kPa at stage 3 hypertension. With the increasing blood pressure from normal to stage 3 hypertension, the stresses at the outer walls of TA and AA increase significantly by 92.4% and 95.4%, respectively. The stresses in SA and RA appear a linear variation through the wall thickness approximately. The increases in blood pressure raise the stresses in the walls of SA and RA to 77.3% and 73.1% on average, respectively. For CCA, a uniform stress distribution is observed in the vessel wall under normal blood pressure, while the stress decreases along the radial direction under hypertensions. The maximum stress at the inner wall of CCA increases by 117.8%, up to 111.0 kPa at stage 3 hypertension.

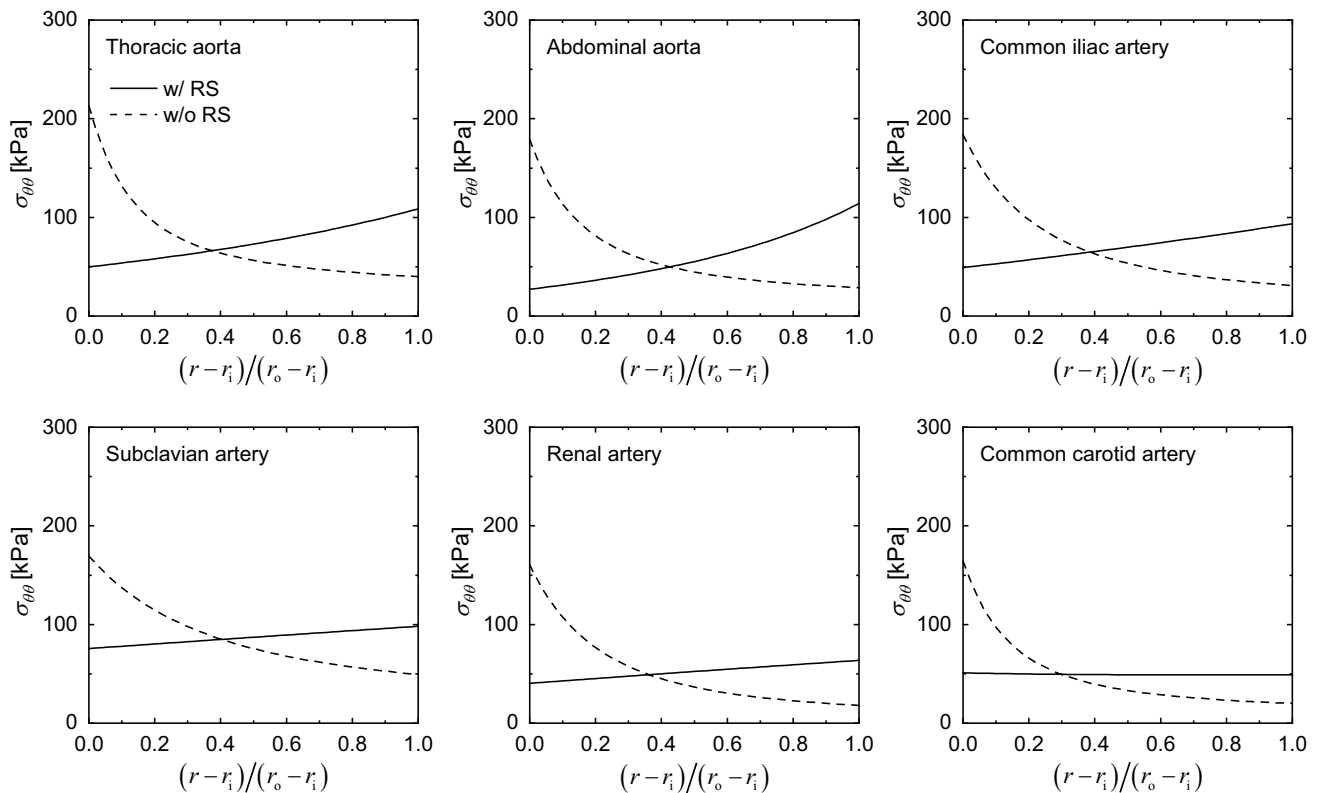


Fig. 2 A comparison of stress distributions $\sigma_{\theta\theta}$ between the results with residual stress (w/RS) and those without residual stress (w/o RS) under normal blood pressure $P=10.8$ kPa. The normalized radius $r_n = (r - r_i) / (r_o - r_i)$ is used as the abscissa, in which $r_n = 0$

denotes the inner radius r_i and $r_n = 1$ denotes the outer radius r_o . The variation of r_n from 0 to 1 represents the change of radial location from the inner wall to the outer wall

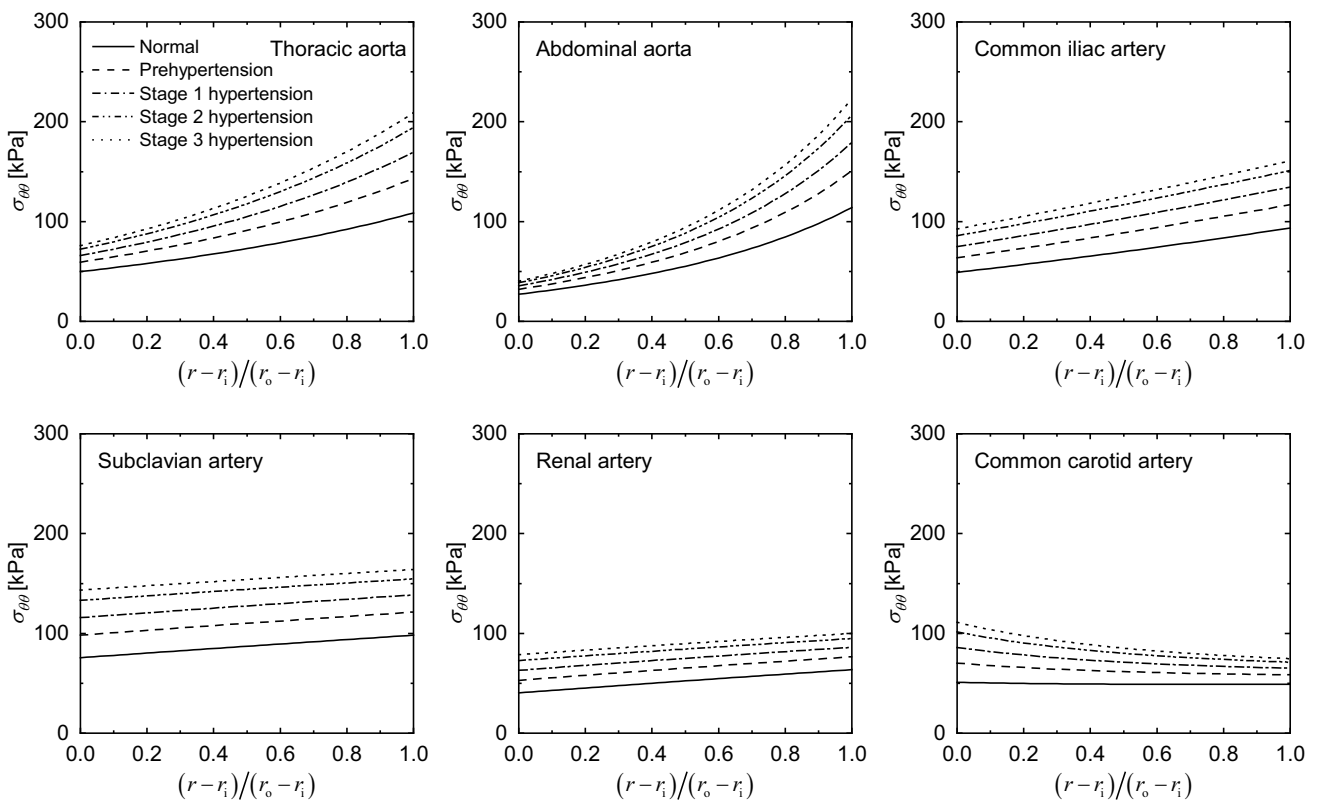


Fig. 3 Distributions of circumferential stresses $\sigma_{\theta\theta}$ through vessel walls. The blood pressure varies from normal ($P=10.8$ kPa) to stage 3 hypertension ($P=17.7$ kPa)

Considering that the stress values on the inner and outer surfaces of vessel walls are of particular interest for current vulnerable plaque research, the stresses of the inner, middle, and outer surfaces of the six blood vessels in Fig. 3 are summarized in Table 3 as a reference. The stress values of both normal pressure (10.8 kPa) and stage 3 hypertension (17.7 kPa) were listed, and their differences are shown in Table 3.

3.3 Strain distributions

Figure 4 illustrates the distributions of the circumferential strains $\epsilon_{\theta\theta}$ across the vessel walls at different

hypertension stages. The strains in TA, AA, and CIA exhibit a mild increase along the radial direction. The maximum strain around 0.41–0.46 is observed at the outer wall of CIA. The strains in SA and RA are around 0.3 and 0.2, respectively, which remain almost constant across the vessel walls. The strain in CCA decreases along the radial direction from the maximum value 0.33 at the inner wall.

The strains of the inner, middle, and outer surfaces of the six blood vessels in Fig. 4 are summarized in Table 4.

Table 3 The stresses (Unit: kPa) of the inner, middle, and outer surfaces of the selected blood vessels under normal blood pressure and hypertension

	Normal: 10.8 kPa			Hypertension: 17.7 kPa		
	Inner	Middle	Outer	Inner	Middle	Outer
TA	49.8	72.9	108.6	75.9	125.3	208.9
AA	27.1	55.2	114.1	40.4	94.1	223.0
CIA	49.1	69.8	93.5	92.5	125.1	160.8
SA	75.6	87.1	98.2	143.4	154.0	164.0
RA	40.3	52.4	63.6	78.6	89.8	99.9
CCA	51.0	49.1	49.1	111.0	85.3	74.5

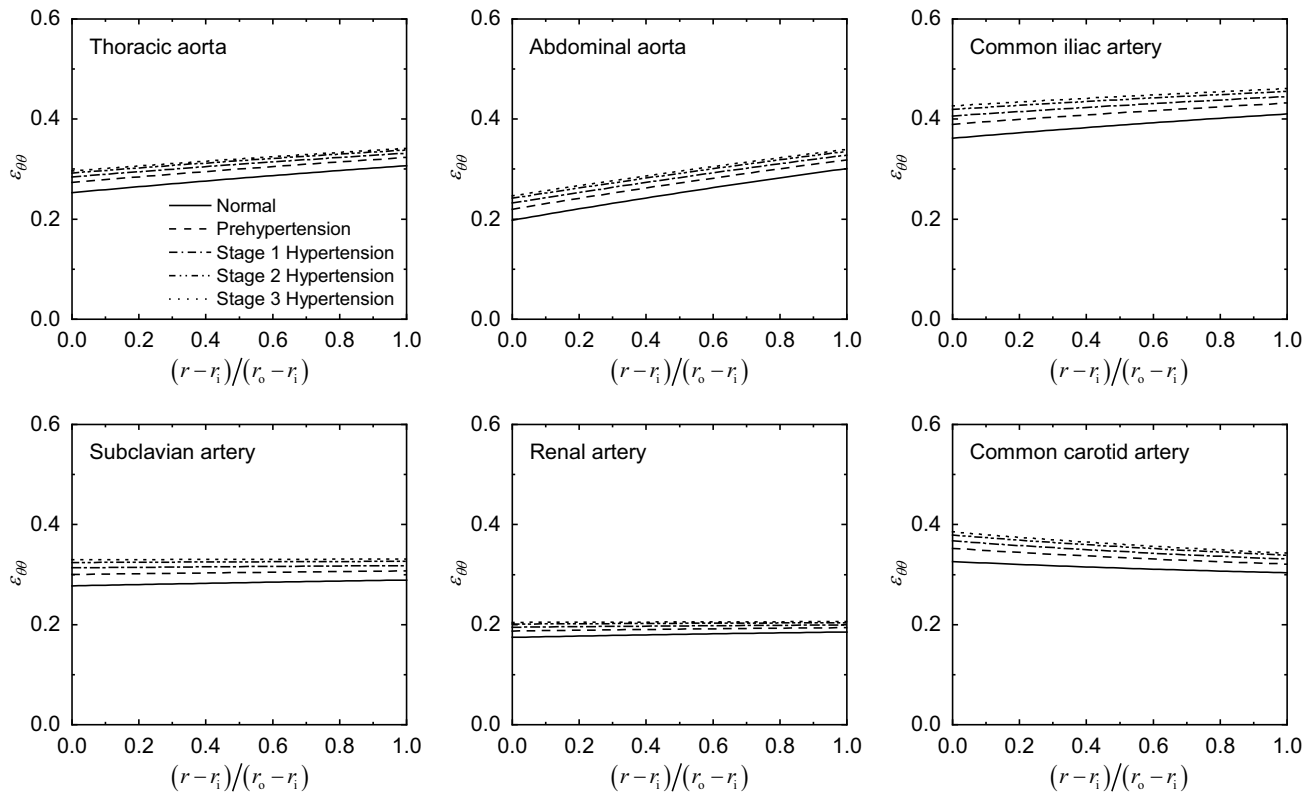


Fig. 4 Distributions of circumferential strains $\epsilon_{\theta\theta}$ through vessel walls. The blood pressure varies from normal ($P=10.8$ kPa) to stage 3 hypertension ($P=17.7$ kPa)

Table 4 The strains of the inner, middle, and outer surfaces of the selected blood vessels under normal blood pressure and hypertension

	Normal: 10.8 kPa			Hypertension: 17.7 kPa		
	Inner	Middle	Outer	Inner	Middle	Outer
TA	0.25	0.28	0.31	0.30	0.32	0.34
AA	0.20	0.25	0.30	0.25	0.30	0.34
CIA	0.36	0.39	0.41	0.43	0.44	0.46
SA	0.28	0.28	0.29	0.33	0.33	0.33
RA	0.17	0.18	0.19	0.20	0.21	0.21
CCA	0.33	0.31	0.30	0.39	0.36	0.34

3.4 Stress gradients

Based on the stress distributions in Fig. 3, the stress gradients $d\sigma_{\theta\theta}/dr$ are plotted against the normalized radius in Fig. 5. In comparison with TA and CIA, the stress gradient of AA increases obviously along the radial direction, which reaches the maximum of 311.6 kPa/mm at the outer wall. Blood pressure increase strongly affects the stress gradient at the outer wall of AA. The stress gradients in SA and RA decrease slightly along the radial direction, and all of them are less than 40.0 kPa/mm. The stress gradient in the wall of CCA is found to be negative which decreases rapidly near the inner wall and then approaches to a constant near the outer wall. A lowest

value of -91.5 kPa/mm is observed at the inner wall of CCA at stage 3 hypertension.

4 Discussions

Although lots of experiments for vascular cells in vitro have been reported in the studies of mechano-transduction, detailed examinations of the applied mechanical niches for cells, namely the stresses and strains comparing to their in vivo background, have not attracted sufficient attention yet. Benefiting from the progress in measuring the mechanical properties of human blood vessels (Kamenskiy et al. 2014), this study further evaluated three key mechanical

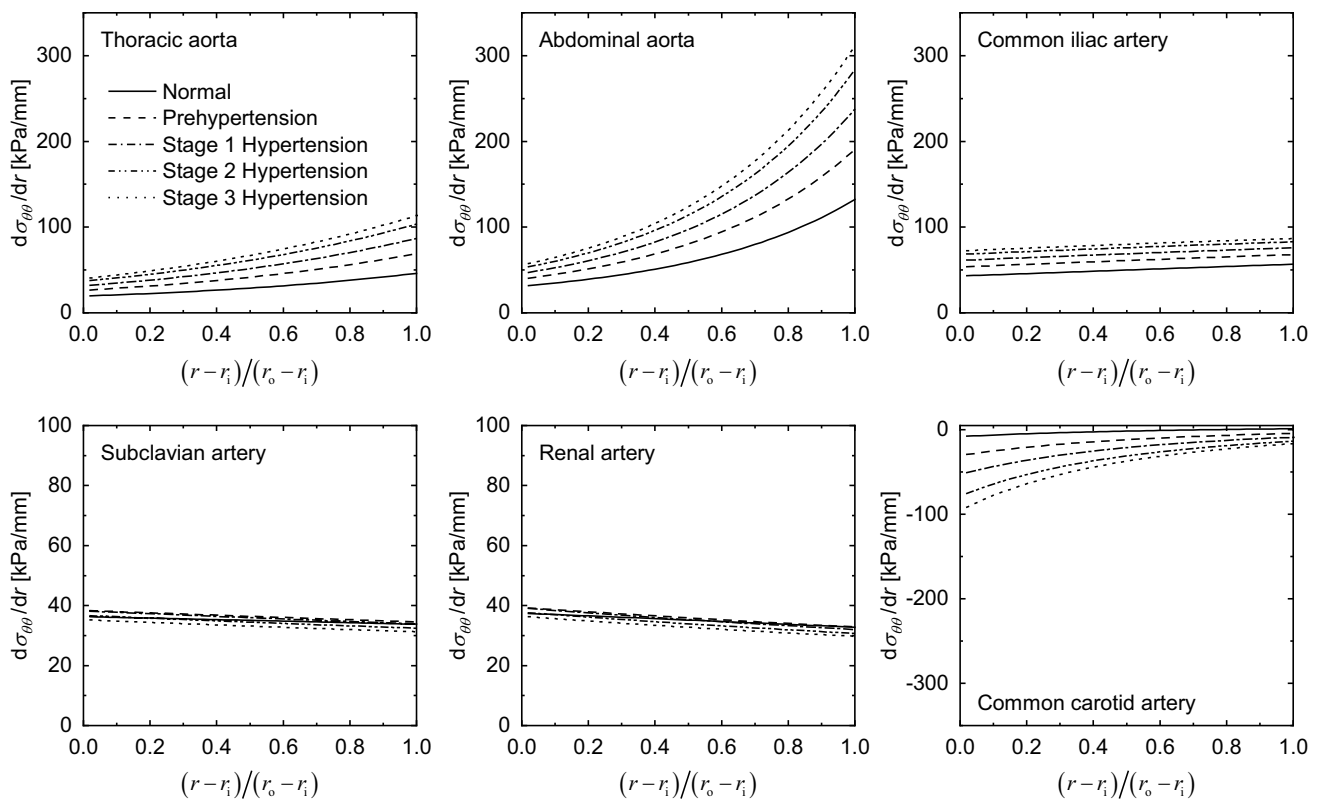


Fig. 5 Distributions of circumferential stress gradients $d\sigma_{\theta\theta}/dr$ through vessel walls. The blood pressure varies from normal ($P=10.8$ kPa) to stage 3 hypertension ($P=17.7$ kPa)

factors, namely the mechanical stress, strain, and stress gradient, which constitute the mechanical niches of vascular cells and provide a site-specific mechanical reference for in vitro experiments.

4.1 “Site-specific” and “disease-specific” related biomechanical characteristics

In Fig. 3, three distinct characteristics of stress distribution were observed in the walls of the six selected blood vessels. In TA, AA, and CIA, the stresses increase along the radial direction. In contrast, the stresses decrease in CCA. In SA and RA, the stresses present relatively uniform distributions. Similar characteristics of strain distribution were also observed in the vessel walls, as shown in Fig. 4.

Higher strains on the inner surface of CCA may trigger the extracellular matrix (ECM) turnover (O’Callaghan and Williams 2000) and receptor-mediated apoptosis of the vascular smooth muscle cells (VSMCs) (Cattaruzza et al. 2000; Sotoudeh et al. 2002) and explain the inflammatory response initiated by the dysfunction of the endothelial cells (ECs) (Xiong et al. 2013; Spescha et al. 2014). In contrast, excessive stretch on the outer surface of TA, AA, and CIA may regulate the cytoskeletal remodeling and cell reorientation

of fibroblasts (Yoshigi et al. 2005; Faust et al. 2011) and support the “outside-in” inflammation hypothesis initiated by the aortic adventitial fibroblasts (Maiellaro and Taylor 2007; Tieu et al. 2011; Michel et al. 2011; Libby and Hansson 2015).

4.2 Spatial gradient of mechanical stresses as a novel mechanical factor

As illustrated in Fig. 5, different stress gradients appeared in different vessel walls as the “site-specific” mechanical stresses and strains, which suggested that the stress gradient should be considered as a novel mechanical factor in mechano-biological studies.

It was found that relatively large stress gradient appeared at the outer surface of AA (311.6 kPa/mm), which was one order of magnitude higher than those of SA and RA. The increase in blood pressure significantly enhanced the stress gradient on the inner surface of CCA and the outer surface of TA and AA. Spatial gradients of mechanical stresses indicate that even slight dislocation of single vascular cells from their rest places could change the mechanical factors around them. As a consequence, the cell–cell and cell–ECM interactions may not only appreciate the local mechanical

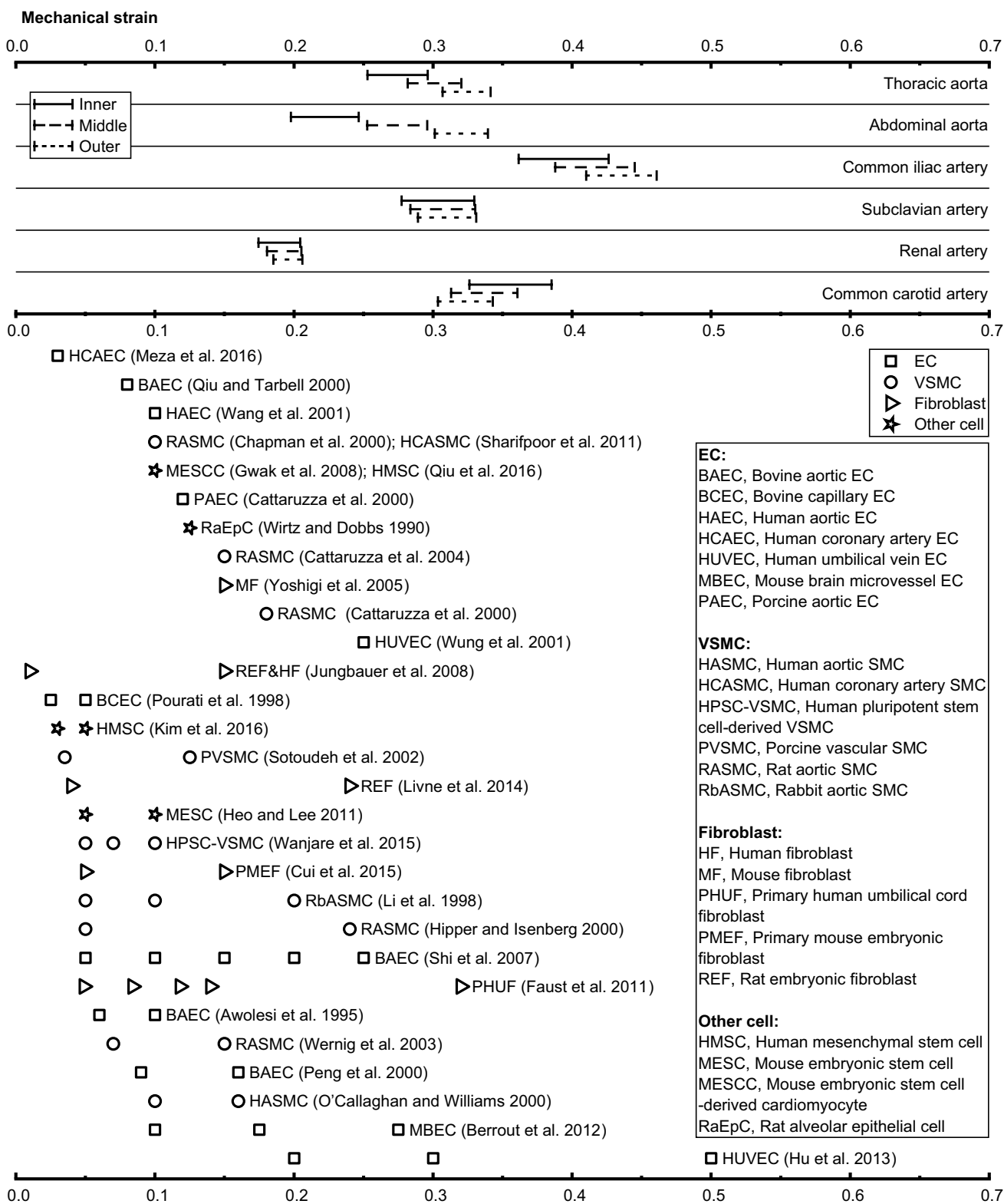


Fig. 6 Mechanical strains on the inner, middle, and outer surfaces of the vessel walls for the six blood vessels, which are correlated with the strains of cell stretching in the literature. ECs (square),

VSMCs (circle), fibroblasts (triangle), and other cells (star) are frequently used in experiments. The blood pressure varies from normal ($P = 10.8$ kPa) to stage 3 hypertension ($P = 17.7$ kPa)

equilibrium of each cells (Maruthamuthu et al. 2011; Doyle et al. 2015), but also the physiological or pathological changes involving proliferation, differentiation or apoptosis of vascular cells that should be considered as dynamic processes coupled with cell behaviors such as migration, rather than static processes confined within isolated regions.

It should be noticed that three-dimensional matrices are of crucial importance in cell adhesion (Cukierman et al. 2001), which drive different cell behaviors versus two-dimensional environments in migration strategies and gene expression (Pedersen and Swartz 2005). From a mechanical point of view, three-dimensional matrices with proper spatial gradients of mechanical factors are helpful to rebuild the microenvironments of vascular tissues and improve the understanding of the dynamic coupling of cell biology with migration.

4.3 Current mechanical references for cell stretching in mechano-biological study

As illustrated in Fig. 6, the mechanical stretches for cell treatment reported in the literature were compared with the strains predicted in the six blood vessels. The strains at the inner, middle, and outer regions of the vessel walls were illustrated to characterize the strains for ECs, VSMCs, and fibroblasts, respectively. The mechanical strains in this study varied within the range of 0.17 to 0.46, but the applied mechanical stretches documented in the literature were mainly within the range of 0.05 to 0.25 for different types of cells, such as for ECs (Awolesi et al. 1995; Pourati et al. 1998; Qiu and Tarbell 2000; Cattaruzza et al. 2000; Peng et al. 2000; Wung et al. 2001; Wang et al. 2001; Shi et al. 2007; Berrout et al. 2012; Hu et al. 2013; Meza et al. 2016), for VSMCs (Li et al. 1998; Hipper and Isenberg 2000; Chapman et al. 2000; Cattaruzza et al. 2000, 2004; O'Callaghan and Williams 2000; Sotoudeh et al. 2002; Wernig et al. 2003; Sharifpoor et al. 2011; Wanjare et al. 2015), for fibroblasts (Yoshigi et al. 2005; Jungbauer et al. 2008; Faust et al. 2011; Livne et al. 2014; Cui et al. 2015), and for other cells (Wirtz and Dobbs 1990; Gwak et al. 2008; Heo and Lee 2011; Kim et al. 2016; Qiu et al. 2016). In some experiments, mechanical stretches were far outside the physiological range (≥ 1.2) for vascular cells (Yamada et al. 2000; Xiong et al. 2013).

The predicted stresses and strains in this study have considered the effect of residual stresses by assuming the opened-up sectors of the blood vessels as the stress-free configuration. The extra stresses or strains reserved by the residual stresses of blood vessels are often excluded in experiments for cells in vitro, so as the relative strains measured clinically. In order to interpret cellular responses more

closely to their in vivo conditions, the absolute strains as presented in this work should be referenced.

5 Conclusions

In this study, we investigated the mechanical environments of vascular cells in six selected human blood vessels in order to illustrate the differences of reported studies of vascular cell mechano-transductions with in vivo mechanical niches of vascular cells and explore novel mechanical factors for in vitro cellular experiments. The results suggest that “disease-specific” dysfunctions of vascular cells should be investigated according to the “site-specific” mechanical environments. In addition to the mechanical stresses and strains, their spatial gradients are important mechanical factors when studying force-regulated cell behaviors. Exploring “factor-specific” mechano-transductions is one prerequisite for the development of vascular cell mechano-biology and tissue engineering.

Acknowledgements This work was supported by the National Natural Science Foundation of China (Grant Numbers 11872040 and 11232010).

Compliance with ethical standards

Conflict of interest The authors declare that they have no conflict of interest.

Appendix 1: Stress responses of blood vessels

It is well known that residual stress exists in the unloaded segment of blood vessels (Vaishnav and Vossoughi 1983; Chuong and Fung 1983). According to (Fung and Liu 1989; Han and Fung 1996), the segment can open up into a (nearly) stress-free sector when radial cutting occurs. Figure 7 illustrates three blood vessel configurations in cylindrical coordinates.

We refer to the stress-free state (Ω_0) of Fig. 7 as the reference configuration. The position $\mathbf{x}_1 \in (\rho, \vartheta, \zeta)$ of a material particle in the unloaded configuration (Ω_1) is

$$\rho = \rho(R), \quad \vartheta = \frac{\pi}{\Theta_0} \Theta, \quad \zeta = \Lambda Z \quad (3)$$

where $\Theta_0 = \pi - \alpha$, the axial stretch ratio $\Lambda = 1.0$ for the assumption of plane strain (Han and Fung 1996).

The deformation gradient of the mapping from the stress-free to unloaded configuration is expressed as

$$\mathbf{F}_1 = \begin{bmatrix} \frac{\partial \rho}{\partial R} & \frac{1}{R} \frac{\partial \rho}{\partial \Theta} & \frac{\partial \rho}{\partial Z} \\ \rho \frac{\partial \vartheta}{\partial R} & \frac{\rho}{R} \frac{\partial \vartheta}{\partial \Theta} & \rho \frac{\partial \vartheta}{\partial Z} \\ \frac{\partial \zeta}{\partial R} & \frac{1}{R} \frac{\partial \zeta}{\partial \Theta} & \frac{\partial \zeta}{\partial Z} \end{bmatrix} = \begin{bmatrix} \frac{\partial \rho}{\partial R} & 0 & 0 \\ 0 & \frac{\pi \rho}{\Theta_0 R} & 0 \\ 0 & 0 & 1 \end{bmatrix}. \quad (4)$$

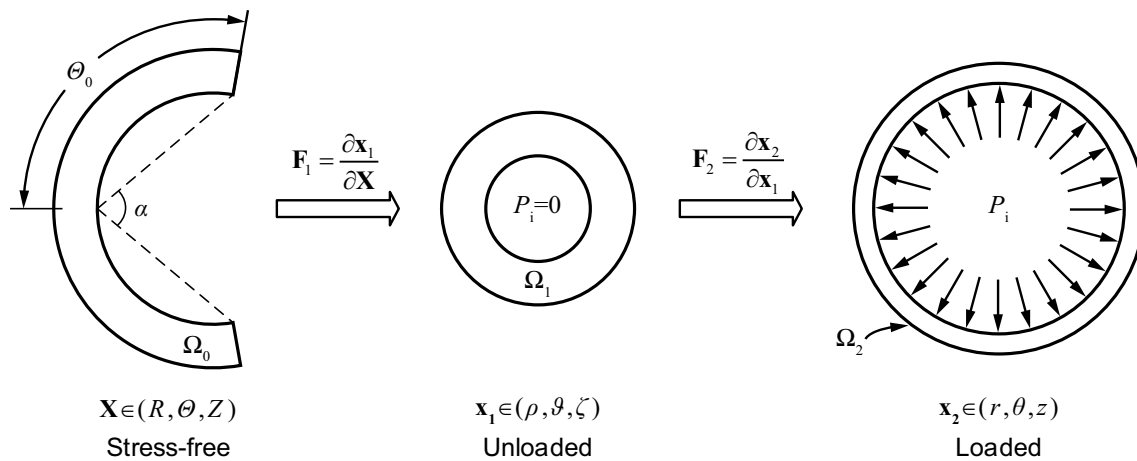


Fig. 7 Three blood vessel configurations in cylindrical coordinates: stress-free (Ω_0) with opening angle α , unloaded (Ω_1), and loaded (Ω_2) with applied blood pressure P_i . The opening angle α is defined by two radii drawn from the midpoint of the inner wall to its tips with $\theta_0 = \pi - \alpha$

Similarly, considering the mapping from the unloaded to loaded configuration, namely $r = r(\rho)$, $\theta = \vartheta + \beta\zeta$, $z = \lambda_z\zeta$, the associated deformation gradient is formulated as

$$\mathbf{F}_2 = \begin{bmatrix} \frac{\partial r}{\partial \rho} & \frac{1}{\rho} \frac{\partial r}{\partial \vartheta} & \frac{\partial r}{\partial \zeta} \\ r \frac{\partial \theta}{\partial \rho} & \frac{r}{\rho} \frac{\partial \theta}{\partial \vartheta} & r \frac{\partial \theta}{\partial \zeta} \\ \frac{\partial z}{\partial \rho} & \frac{1}{\rho} \frac{\partial z}{\partial \vartheta} & \frac{\partial z}{\partial \zeta} \end{bmatrix} = \begin{bmatrix} \frac{\partial r}{\partial \rho} & 0 & 0 \\ 0 & \frac{r}{\rho} & r\beta \\ 0 & 0 & \lambda_z \end{bmatrix}, \quad (5)$$

where β is the twist ratio and λ_z is the axial stretch induced by the in vivo axial loading. As the torsion of the blood vessels is not investigated here, $\beta = 0$.

With respect to the reference (stress-free) configuration, the total deformation gradient for a loaded blood vessel is

$$\mathbf{F} = \mathbf{F}_2 \cdot \mathbf{F}_1 = \begin{bmatrix} \frac{\partial r}{\partial R} & 0 & 0 \\ 0 & \frac{\pi r}{\theta_0 R} & 0 \\ 0 & 0 & \lambda_z \end{bmatrix}. \quad (6)$$

The right and left Cauchy–Green tensors are often used to measure the deformation and are defined as $\mathbf{C} = \mathbf{F}^T \cdot \mathbf{F}$ and $\mathbf{b} = \mathbf{F} \cdot \mathbf{F}^T$, respectively.

In order to describe the incompressibility of the vascular tissues, the constitutive relation $W(\mathbf{C}, \mathbf{M}_i)$ in Eq. (1) is modified as follows:

$$\psi = W(\mathbf{C}, \mathbf{M}_i) - \frac{1}{2}p(I_3 - 1), \quad (7)$$

where the scalar p is the Lagrange multiplier and I_3 is the third invariant of the right Cauchy–Green tensor \mathbf{C} with the constraint $I_3 = 1$.

Using the chain rule, the second Piola–Kirchhoff stress tensor \mathbf{S} is expressed as

$$\mathbf{S} = 2 \frac{\partial \psi}{\partial \mathbf{C}} = 2 \left(\frac{\partial W}{\partial I_1} \frac{\partial I_1}{\partial \mathbf{C}} + \sum_{i=1}^4 \frac{\partial W}{\partial I_{i4}} \frac{\partial I_{i4}}{\partial \mathbf{C}} \right) - p \frac{\partial I_3}{\partial \mathbf{C}}. \quad (8)$$

The derivatives of I_1 , I_3 , and I_{i4} with respect to \mathbf{C} have the following forms

$$\frac{\partial I_1}{\partial \mathbf{C}} = \frac{\partial \text{tr} \mathbf{C}}{\partial \mathbf{C}} = \mathbf{I}, \quad \frac{\partial I_3}{\partial \mathbf{C}} = \frac{\partial \det \mathbf{C}}{\partial \mathbf{C}} = I_3 \mathbf{C}^{-1}, \quad \frac{\partial I_{i4}}{\partial \mathbf{C}} = \frac{\partial (\mathbf{a}_i \cdot \mathbf{C} \mathbf{a}_i)}{\partial \mathbf{C}} = \mathbf{M}_i \quad (9)$$

in which \mathbf{I} is the identity matrix.

Substituting Eq. (9) into (8) results in

$$\mathbf{S} = 2 \left(W_1 \mathbf{I} + \sum_{i=1}^4 W_{i4} \mathbf{M}_i \right) - p \mathbf{C}^{-1}, \quad (10)$$

with $W_1 = \partial W / \partial I_1$, $W_{i4} = \partial W / \partial I_{i4}$.

The Piola transformation of Eq. (10) provides the Cauchy stress tensor as

$$\boldsymbol{\sigma} = J^{-1} \mathbf{F} \mathbf{S} \mathbf{F}^T = \boldsymbol{\sigma}^* - p \mathbf{I} \quad (11)$$

with $\boldsymbol{\sigma}^* = 2 \left(W_1 \mathbf{b} + \sum_{i=1}^4 W_{i4} \mathbf{F} \mathbf{M}_i \mathbf{F}^T \right)$ for the sake of convenience.

Appendix 2: Solving equilibrium equations

Regardless of the body forces, the equilibrium equations can be expressed as

$$\text{div } \boldsymbol{\sigma} = 0. \quad (12)$$

The non-trivial component of Eq. (12) in cylindrical coordinates is

$$\frac{d\sigma_{rr}}{dr} + \frac{1}{r} (\sigma_{rr} - \sigma_{\theta\theta}) = 0. \quad (13)$$

Neglecting the pressure on the outer wall ($P_o = 0$) and considering the internal blood pressure P_i , the boundary conditions are

$$\sigma_{rr}(r_i) = -P_i, \quad \sigma_{rr}(r_o) = 0, \quad (14)$$

where r_i and r_o are the inner and outer radii, respectively.

The integration of Eq. (13) from r_i to r yields

$$\sigma_{rr}(r) - \sigma_{rr}(r_i) = \int_{r_i}^r \frac{1}{r} (\sigma_{\theta\theta} - \sigma_{rr}) dr. \quad (15)$$

Incorporating the stress components of Eq. (11) into (15) leads to the expression of the Lagrange multiplier:

$$p(r) = \sigma_{rr}^*(r) + P_i - \int_{r_i}^r \frac{1}{r} (\sigma_{\theta\theta}^*(r) - \sigma_{rr}^*(r)) dr. \quad (16)$$

With the boundary conditions of Eq. (14), the integration of Eq. (13) from r_i to r_o relates the blood pressure P_i to the vessel wall radial deformation; that is,

$$P_i = \int_{r_i}^{r_o} \frac{1}{r} (\sigma_{\theta\theta}^*(r) - \sigma_{rr}^*(r)) dr. \quad (17)$$

With Eq. (6), the incompressibility requires $\det \mathbf{F} \equiv 1$ and leads to

$$\partial r / \partial R = \Theta_0 R / (\pi r \lambda_z). \quad (18)$$

The integration of Eq. (18) from the inner to outer radius yields

$$r_o^2 - r_i^2 = \frac{\Theta_0}{\pi \lambda_z} (R_o^2 - R_i^2). \quad (19)$$

By solving Eqs. (17) and (19) with the provided data of R_i , R_o , α , P_i , and λ_z , the inner (r_i) and outer (r_o) radii of the loaded configuration are obtained. Subsequently, the Lagrange multiplier $p(r)$ in Eq. (16) can be integrated numerically, following which the stress components in Eq. (11) are determined.

References

- Anwar MA, Shalhoub J, Lim CS et al (2012) The effect of pressure-induced mechanical stretch on vascular wall differential gene expression. *J Vasc Res* 49:463–478. <https://doi.org/10.1159/000339151>
- Awolesi MA, Sessa WC, Sumpio BE (1995) Cyclic strain upregulates nitric oxide synthase in cultured bovine aortic endothelial cells. *J Clin Invest* 96:1449–1454. <https://doi.org/10.1172/JCI118181>
- Azar D, Ohadi D, Rachev A et al (2018) Mechanical and geometrical determinants of wall stress in abdominal aortic aneurysms: a computational study. *PLoS ONE* 13:e0192032. <https://doi.org/10.1371/journal.pone.0192032>

- Berrout J, Jin M, O'Neil RG (2012) Critical role of TRPP2 and TRPC1 channels in stretch-induced injury of blood-brain barrier endothelial cells. *Brain Res* 1436:1–12. <https://doi.org/10.1016/j.brainres.2011.11.044>
- Boileau E, Nithiarasu P, Blanco PJ et al (2015) A benchmark study of numerical schemes for one-dimensional arterial blood flow modelling. *Int J Numer Method Biomed Eng* 31:1–33. <https://doi.org/10.1002/cnm.2732>
- Boutouyrie P, Laurent S, Benetos A et al (1992) Opposing effects of ageing on distal and proximal large arteries in hypertensives. *J Hypertens Suppl* 10:S87–S91
- Cattaruzza M, Dimigen C, Ehrenreich H, Hecker M (2000) Stretch-induced endothelin B receptor-mediated apoptosis in vascular smooth muscle cells. *FASEB J* 14:991–998
- Cattaruzza M, Lattrich C, Hecker M (2004) Focal adhesion protein zyxin is a mechanosensitive modulator of gene expression in vascular smooth muscle cells. *Hypertension* 43:726–730. <https://doi.org/10.1161/01.HYP.0000119189.82659.52>
- Chapman GB, Durante W, Hellums JD, Schafer AI (2000) Physiological cyclic stretch causes cell cycle arrest in cultured vascular smooth muscle cells. *Am J Physiol Heart Circ Physiol* 278:H748–H754
- Chen CS (2008) Mechanotransduction—a field pulling together? *J Cell Sci* 121:3285–3292. <https://doi.org/10.1242/jcs.023507>
- Chobanian AV, Bakris GL, Black HR et al (2003) Seventh report of the joint national committee on prevention, detection, evaluation, and treatment of high blood pressure. *Hypertension* 42:1206–1252. <https://doi.org/10.1161/01.HYP.0000107251.49515.c2>
- Chuong CJ, Fung YC (1983) Three-dimensional stress distribution in arteries. *J Biomech Eng* 105:268–274. <https://doi.org/10.1115/1.3138417>
- Chuong CJ, Fung YC (1986) On residual stresses in arteries. *J Biomech Eng* 108:189–192. <https://doi.org/10.1115/1.3138600>
- Cui Y, Hameed FM, Yang B et al (2015) Cyclic stretching of soft substrates induces spreading and growth. *Nat Commun* 6:6333. <https://doi.org/10.1038/ncomms7333>
- Cukierman E, Pankov R, Stevens DR, Yamada KM (2001) Taking cell-matrix adhesions to the third dimension. *Science* 294:1708–1712. <https://doi.org/10.1126/science.1064829>
- Delfino A, Stergiopoulos N, Moore JE, Meister JJ (1997) Residual strain effects on the stress field in a thick wall finite element model of the human carotid bifurcation. *J Biomech* 30:777–786. [https://doi.org/10.1016/s0021-9290\(97\)00025-0](https://doi.org/10.1016/s0021-9290(97)00025-0)
- Doyle AD, Carvajal N, Jin A et al (2015) Local 3D matrix microenvironment regulates cell migration through spatiotemporal dynamics of contractility-dependent adhesions. *Nat Commun* 6:8720. <https://doi.org/10.1038/ncomms9720>
- Faust U, Hampe N, Rubner W et al (2011) Cyclic stress at mHz frequencies aligns fibroblasts in direction of zero strain. *PLoS ONE* 6:e28963. <https://doi.org/10.1371/journal.pone.0028963>
- Fung YC (1991) What are the residual stresses doing in our blood vessels? *Ann Biomed Eng* 19:237–249. <https://doi.org/10.1007/BF02584301>
- Fung Y-C (1993) *Biomechanics*, 2nd edn. Springer, New York
- Fung YC, Liu SQ (1989) Change of residual strains in arteries due to hypertrophy caused by aortic constriction. *Circ Res* 65:1340–1349. <https://doi.org/10.1161/01.RES.65.5.1340>
- Gasser TC, Schulze-Bauer CAJ, Holzapfel GA (2002) A three-dimensional finite element model for arterial clamping. *J Biomech Eng* 124:355–363. <https://doi.org/10.1115/1.1485284>
- Gasser TC, Auer M, Labruto F et al (2010) Biomechanical rupture risk assessment of abdominal aortic aneurysms: model complexity versus predictability of finite element simulations. *Eur J Vasc Endovasc Surg* 40:176–185. <https://doi.org/10.1016/j.ejvs.2010.04.003>

- Gwak SJ, Bhang SH, Kim IK et al (2008) The effect of cyclic strain on embryonic stem cell-derived cardiomyocytes. *Biomaterials* 29:844–856. <https://doi.org/10.1016/j.biomaterials.2007.10.050>
- Han HC, Fung YC (1996) Direct measurement of transverse residual strains in aorta. *Am J Physiol* 270:H750–H759
- Heo JS, Lee JC (2011) Beta-catenin mediates cyclic strain-stimulated cardiomyogenesis in mouse embryonic stem cells through ROS-dependent and integrin-mediated PI3 K/Akt pathways. *J Cell Biochem* 112:1880–1889. <https://doi.org/10.1002/jcb.23108>
- Hipper A, Isenberg G (2000) Cyclic mechanical strain decreases the DNA synthesis of vascular smooth muscle cells. *Pflugers Arch* 440:19–27
- Holzapfel GA (2000) *Nonlinear solid mechanics. A continuum approach for engineering*. Wiley, Chichester
- Holzapfel GA, Gasser TC, Ogden RW (2000) A new constitutive framework for arterial wall mechanics and a comparative study of material models. *J Elast* 61:1–48. <https://doi.org/10.1023/A:1010835316564>
- Holzapfel GA, Sommer G, Auer M et al (2007) Layer-specific 3D residual deformations of human aortas with non-atherosclerotic intimal thickening. *Ann Biomed Eng* 35:530–545. <https://doi.org/10.1007/s10439-006-9252-z>
- Hu Z, Xiong Y, Han X et al (2013) Acute mechanical stretch promotes eNOS activation in venous endothelial cells mainly via PKA and Akt pathways. *PLoS ONE* 8:e71359. <https://doi.org/10.1371/journal.pone.0071359>
- Humphrey JD (2002) *Cardiovascular solid mechanics: cells, tissues, and organs*. Springer, New York
- Humphrey JD, Holzapfel GA (2012) Mechanics, mechanobiology, and modeling of human abdominal aorta and aneurysms. *J Biomech* 45:805–814. <https://doi.org/10.1016/j.jbiomech.2011.11.021>
- Humphrey JD, Dufresne ER, Schwartz MA (2014) Mechanotransduction and extracellular matrix homeostasis. *Nat Rev Mol Cell Biol* 15:802–812. <https://doi.org/10.1038/nrm3896>
- Ingber DE (2003) Mechanobiology and diseases of mechanotransduction. *Ann Med* 35:564–577. <https://doi.org/10.1080/07853890310016333>
- Isnard RN, Pannier BM, Laurent S et al (1989) Pulsatile diameter and elastic modulus of the aortic arch in essential hypertension: a noninvasive study. *J Am Coll Cardiol* 13:399–405. [https://doi.org/10.1016/0735-1097\(89\)90518-4](https://doi.org/10.1016/0735-1097(89)90518-4)
- Jungbauer S, Gao H, Spatz JP, Kemkemer R (2008) Two characteristic regimes in frequency-dependent dynamic reorientation of fibroblasts on cyclically stretched substrates. *Biophys J* 95:3470–3478. <https://doi.org/10.1529/biophysj.107.128611>
- Kamenskiy AV, Dzenis YA, Kazmi SAJ et al (2014) Biaxial mechanical properties of the human thoracic and abdominal aorta, common carotid, subclavian, renal and common iliac arteries. *Biomech Model Mechanobiol* 13:1341–1359. <https://doi.org/10.1007/s10237-014-0576-6>
- Kim DH, Heo SJ, Kang YG et al (2016) Shear stress and circumferential stretch by pulsatile flow direct vascular endothelial lineage commitment of mesenchymal stem cells in engineered blood vessels. *J Mater Sci Mater Med* 27:1–11. <https://doi.org/10.1007/s10856-016-5670-0>
- Kumar A, Placone JK, Engler AJ (2017) Understanding the extracellular forces that determine cell fate and maintenance. *Development* 144:4261–4270. <https://doi.org/10.1242/dev.158469>
- Lally C, Dolan F, Prendergast PJ (2005) Cardiovascular stent design and vessel stresses: a finite element analysis. *J Biomech* 38:1574–1581. <https://doi.org/10.1016/j.jbiomech.2004.07.022>
- Li Q, Muragaki Y, Hatamura I et al (1998) Stretch-induced collagen synthesis in cultured smooth muscle cells from rabbit aortic media and a possible involvement of angiotensin II and transforming growth factor-beta. *J Vasc Res* 35:93–103. <https://doi.org/10.1159/000025570>
- Libby P, Hansson GK (2015) Inflammation and immunity in diseases of the arterial tree: players and layers. *Circ Res* 116:307–311. <https://doi.org/10.1161/CIRCRESAHA.116.301313>
- Livne A, Bouchbinder E, Geiger B (2014) Cell reorientation under cyclic stretching. *Nat Commun* 5:3938. <https://doi.org/10.1038/ncomms4938>
- Lo CM, Wang HB, Dembo M, Wang YL (2000) Cell movement is guided by the rigidity of the substrate. *Biophys J* 79:144–152. [https://doi.org/10.1016/S0006-3495\(00\)76279-5](https://doi.org/10.1016/S0006-3495(00)76279-5)
- Maiellaro K, Taylor WR (2007) The role of the adventitia in vascular inflammation. *Cardiovasc Res* 75:640–648. <https://doi.org/10.1016/j.cardiores.2007.06.023>
- Maruthamuthu V, Sabass B, Schwarz US, Gardel ML (2011) Cell-ECM traction force modulates endogenous tension at cell-cell contacts. *Proc Natl Acad Sci* 108:4708–4713. <https://doi.org/10.1073/pnas.1011123108>
- Masson I, Beaussier H, Boutouyrie P et al (2011) Carotid artery mechanical properties and stresses quantified using in vivo data from normotensive and hypertensive humans. *Biomech Model Mechanobiol* 10:867–882. <https://doi.org/10.1007/s10237-010-0279-6>
- Meza D, Abejar L, Rubenstein DA, Yin W (2016) A shearing-stretching device that can apply physiological fluid shear stress and cyclic stretch concurrently to endothelial cells. *J Biomech Eng* 138:031007. <https://doi.org/10.1115/1.4032550>
- Michel JB, Martin-Ventura JL, Egido J et al (2011) Novel aspects of the pathogenesis of aneurysms of the abdominal aorta in humans. *Cardiovasc Res* 90:18–27. <https://doi.org/10.1093/cvr/cvq337>
- O’Callaghan CJ, Williams B (2000) Mechanical strain-induced extracellular matrix production by human vascular smooth muscle cells: role of TGF-1. *Hypertension* 36:319–324. <https://doi.org/10.1161/01.HYP.36.3.319>
- Pedersen JA, Swartz MA (2005) Mechanobiology in the third dimension. *Ann Biomed Eng* 33:1469–1490. <https://doi.org/10.1007/s10439-005-8159-4>
- Peng X, Recchia FA, Byrne BJ et al (2000) In vitro system to study realistic pulsatile flow and stretch signaling in cultured vascular cells. *Am J Physiol Cell Physiol* 279:C797–C805. <https://doi.org/10.1152/ajpcell.2000.279.3.C797>
- Pierce DM, Fastl TE, Rodriguez-Vila B et al (2015) A method for incorporating three-dimensional residual stretches/stresses into patient-specific finite element simulations of arteries. *J Mech Behav Biomed Mater* 47:147–164. <https://doi.org/10.1016/j.jmbm.2015.03.024>
- Pourati J, Maniotis A, Spiegel D et al (1998) Is cytoskeletal tension a major determinant of cell deformability in adherent endothelial cells? *Am J Physiol* 274:C1283–C1289. <https://doi.org/10.1152/ajpcell.1998.274.5.C1283>
- Qiu Y, Tarbell JM (2000) Interaction between wall shear stress and circumferential strain affects endothelial cell biochemical production. *J Vasc Res* 37:147–157. <https://doi.org/10.1159/000025726>
- Qiu Y, Lei J, Koob TJ, Temenoff JS (2016) Cyclic tension promotes fibroblastic differentiation of human MSCs cultured on collagen-fibre scaffolds. *J Tissue Eng Regen Med* 10:989–999. <https://doi.org/10.1002/term.1880>
- Saini A, Berry C, Greenwald S (1995) Effect of age and sex on residual stress in the aorta. *J Vasc Res* 32:398–405. <https://doi.org/10.1159/000159115>
- Schulze-Bauer CAJ, Mörth C, Holzapfel GA (2003) Passive biaxial mechanical response of aged human iliac arteries. *J Biomech Eng* 125:395. <https://doi.org/10.1115/1.1574331>
- Sears C, Kaunas R (2016) The many ways adherent cells respond to applied stretch. *J Biomech* 49:1347–1354. <https://doi.org/10.1016/j.jbiomech.2015.10.014>

- Sharifpoor S, Simmons CA, Labow RS, Paul Santerre J (2011) Functional characterization of human coronary artery smooth muscle cells under cyclic mechanical strain in a degradable polyurethane scaffold. *Biomaterials* 32:4816–4829. <https://doi.org/10.1016/j.biomaterials.2011.03.034>
- Sheetz M, Yu H (2018) *The cell as a machine, illustrate*. Cambridge University Press, Cambridge
- Shi F, Chiu YJ, Cho Y et al (2007) Down-regulation of ERK but not MEK phosphorylation in cultured endothelial cells by repeated changes in cyclic stretch. *Cardiovasc Res* 73:813–822. <https://doi.org/10.1016/j.cardiores.2006.12.014>
- Sommer G, Benedikt C, Niestrawska JA et al (2018) Mechanical response of human subclavian and iliac arteries to extension, inflation and torsion. *Acta Biomater* 75:235–252. <https://doi.org/10.1016/j.actbio.2018.05.043>
- Sotoudeh M, Li Y-S, Yajima N et al (2002) Induction of apoptosis in vascular smooth muscle cells by mechanical stretch. *Am J Physiol Heart Circ Physiol* 282:H1709–H1716. <https://doi.org/10.1152/ajpheart.00744.2001>
- Spescha RD, Glanzmann M, Simic B et al (2014) Adaptor protein p66Shc mediates hypertension-associated, cyclic stretch-dependent, endothelial damage. *Hypertension* 64:347–353. <https://doi.org/10.1161/HYPERTENSIONAHA.113.02129>
- Tieu BC, Ju X, Lee C et al (2011) Aortic adventitial fibroblasts participate in angiotensin-induced vascular wall inflammation and remodeling. *J Vasc Res* 48:261–272. <https://doi.org/10.1159/000320358>
- Vaishnav RN, Vossoughi J (1983) Estimation of residual strains in aortic segments. *Biomed Eng II* 2:330–333. <https://doi.org/10.1016/B978-0-08-030145-7.50078-7>
- Wang JHC, Goldschmidt-Clermont P, Wille J, Yin FCP (2001) Specificity of endothelial cell reorientation in response to cyclic mechanical stretching. *J Biomech* 34:1563–1572. [https://doi.org/10.1016/S0021-9290\(01\)00150-6](https://doi.org/10.1016/S0021-9290(01)00150-6)
- Wang Q, Canton G, Guo J et al (2017) MRI-based patient-specific human carotid atherosclerotic vessel material property variations in patients, vessel location and long-term follow up. *PLoS ONE* 12:e0180829. <https://doi.org/10.1371/journal.pone.0180829>
- Wanjare M, Agarwal N, Gerecht S (2015) Biomechanical strain induces elastin and collagen production in human pluripotent stem cell-derived vascular smooth muscle cells. *Am J Physiol Cell Physiol* 309:C271–C281. <https://doi.org/10.1152/ajpccell.00366.2014>
- Wells RG (2008) The role of matrix stiffness in regulating cell behavior. *Hepatology* 47:1394–1400. <https://doi.org/10.1002/hep.22193>
- Wernig F, Mayr M, Xu Q (2003) Mechanical stretch-induced apoptosis in smooth muscle cells is mediated by beta1-integrin signaling pathways. *Hypertension* 41:903–911. <https://doi.org/10.1161/01.HYP.0000062882.42265.88>
- Wirtz H, Dobbs L (1990) Calcium mobilization and exocytosis after one mechanical stretch of lung epithelial cells. *Science* 250:1266–1269. <https://doi.org/10.1126/science.2173861>
- Wung BS, Cheng JJ, Shyue S-K, Wang DL (2001) NO modulates monocyte chemotactic protein-1 expression in endothelial cells under cyclic strain. *Arter Thromb Vasc Biol* 21:1941–1947. <https://doi.org/10.1161/hq1201.099428>
- Xiong Y, Hu Z, Han X et al (2013) Hypertensive stretch regulates endothelial exocytosis of Weibel-Palade bodies through VEGF receptor 2 signaling pathways. *Cell Res* 23:820–834. <https://doi.org/10.1038/cr.2013.56>
- Yamada T, Naruse K, Sokabe M (2000) Stretch-induced morphological changes of human endothelial cells depend on the intracellular level of Ca²⁺ + rather than of cAMP. *Life Sci* 67:2605–2613. [https://doi.org/10.1016/S0024-3205\(00\)00844-4](https://doi.org/10.1016/S0024-3205(00)00844-4)
- Yoshigi M, Hoffman LM, Jensen CC et al (2005) Mechanical force mobilizes zyxin from focal adhesions to actin filaments and regulates cytoskeletal reinforcement. *J Cell Biol* 171:209–215. <https://doi.org/10.1083/jcb.200505018>

Publisher's Note Springer Nature remains neutral with regard to jurisdictional claims in published maps and institutional affiliations.